

Indentation and Gradient Elasticity

by

Avraam Konstantinidis

Lecture Abstract

First, indentation basics are presented through a flash-back to the test's development from its origin in the beginning of the 19th century, until now. Some of the test's shortcomings are also discussed and an alternative way of handling indentation (load vs. depth) data is proposed. It starts from the simple assumption that the displacement profile underneath a pyramidal (Berkovich/Vickers) tip for very shallow indents may be approximated by Boussinesq's classical solution, while for deeper ones it should be determined in connection with the tip's specific geometry. With the above assumption for the displacement field in the neighborhood of the indenter, corresponding expressions for the strain are deduced, while the local stress is assumed to vary linearly with strain and its gradient, utilizing the Gradient Elasticity theory. The so-calculated stress components, as well as the von Mises equivalent stress, turn out to be parametric functions of the material's constants modeling elasticity (Young's modulus, Poisson's ratio) and inhomogeneity (gradient coefficient or internal length) as well as of the maximum elastic displacement value (coming from the Boussinesq's solution) of strain. By properly adjusting these parameters, the proposed formulation seems to be able to predict the mechanical response of the material underneath the indenter for the specific pyramidal tip geometry (Berkovich or Vickers).

A. Konstantinidis' Short CV



Avraam A. Konstantinidis received his Diploma in Electrical Engineering in 1996 as well as his PhD in 2000 (with Prof. E.C. Aifantis as his advisor), respectively, from the Aristotle University of Thessaloniki (AUTH). In 2003 he joined the General Department of AUTH, as a Lecturer and later as an Assistant Professor, and he is currently an Associate Professor of the Civil Engineering Department of AUTH and also acts as the Director of the Laboratory of Engineering Mechanics of AUTH (<http://etem.civil.auth.gr/en/>). His research interests involve non-local modeling of material behavior at various scales (macro-, micro- and nano-scale), experiments for material characterization at the micro- and nano-scale (nanoindentation, micro-tension, confocal microscopy), as well as multiscale and hybrid gradient-stochastic simulations. He has published over 50 journal, as well as 15 proceedings articles, and his work has received ~330 citations and an h-index of 10 (SCOPUS).

Representative Publications

Konstantinidis A.A., Aifantis K.E. and De Hosson J.Th.M., Capturing the stochastic mechanical behavior of micro and nanopillars, *Mater. Sci. Eng. A* **597**, 89-94, 2014.

Kampouris A.K., Konstantinidis A.A., Yang R., Bai Y. and Aifantis E.C., Internal length gradient approach to pyramidal/spherical nanoindentation experiments, *Nanoscience and Technology* **13**, 47-66, 2022.

Konstantinidis, A. and Aifantis, E.C., Gradients and internal lengths in small scale problems of mechanics, *Int. J. Multisc. Computat. Engng.* **20**, 89-110, 2022.

Indentation and Gradient Elasticity

A.A. Konstantinidis

*Laboratory of Engineering Mechanics
School of Civil Engineering
Aristotle University, Thessaloniki 54124, Greece
<http://etem.civil.auth.gr/en/>*

MICRO- & NANO- INDENTATION

■ Hardness Measurement with Indentation

- *Hardness* $H = \frac{P}{A_C}$; P : Applied Load A_C : Contact Area

- *Hardness Tests*

- *Brinell Test (1900)*

- A 10-mm diameter hardened steel or carbide ball is pushed into the surface of the material, with a 3000 kgf (~30 kN) imposed load. The depth to which the ball penetrates the material surface is an indication of the *Brinell Hardness Number*

- *Vickers Test (1921)*

- The indenter shape should be capable of producing geometrically similar impressions, irrespective of size, with the impression having well-defined points of measurement; and the indenter should be hard to deform. A diamond in the form of a square-based pyramid satisfied these conditions.

- ***Meyer Hardness***

Meyer hardness is defined as the applied load over the projected contact area

$$HM = \frac{P}{A_p} \quad A_p: \text{ Projected area}$$

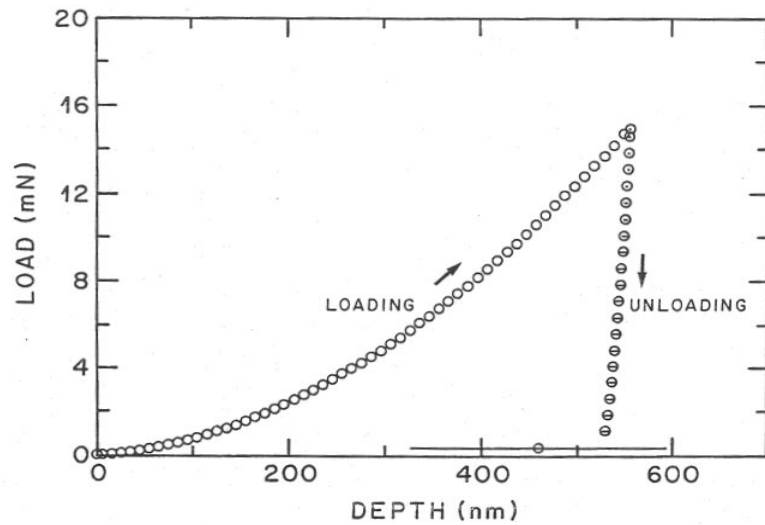
- ***Relation between HM and Yield Stress (Tabor 1951)***

The significance of the hardness value is due to the simple relationship between Meyer hardness and yield stress

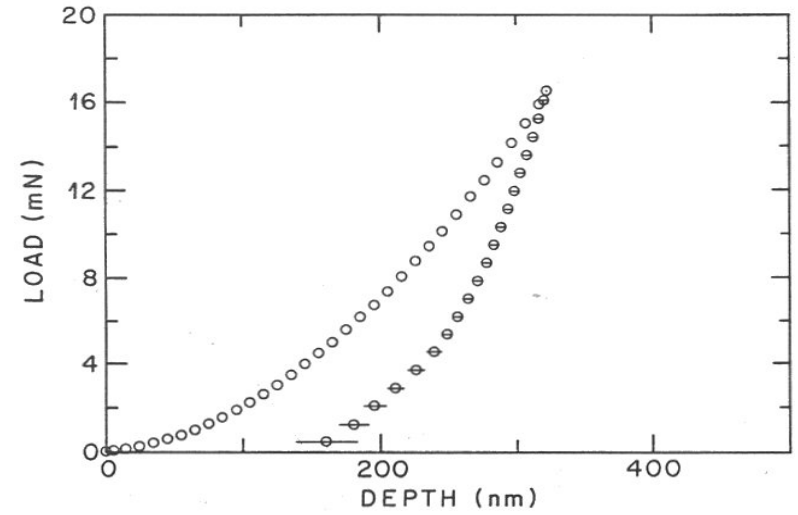
$$HM = 3 \sigma_y$$

- ***Problems concerning the interpretation of indentation data***

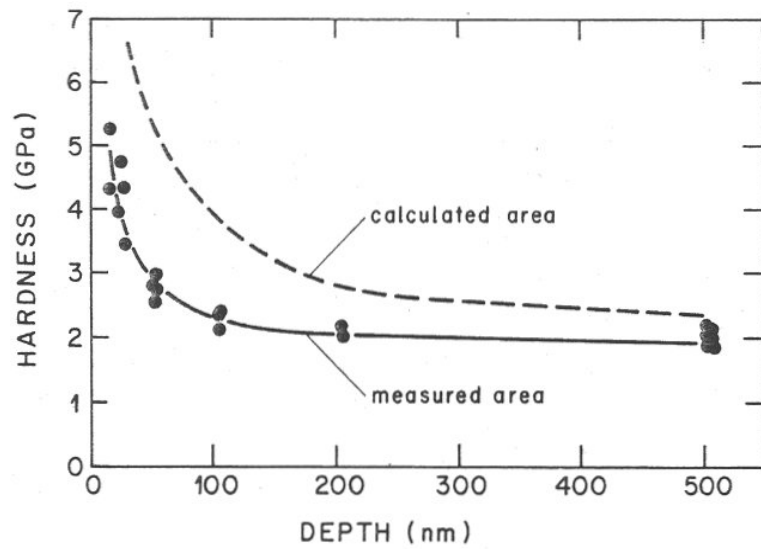
1. Measured hardness increases with decreasing depth of indentation for very small indents.
2. Some materials exhibit a significant amount of elastic strain during deformation under the tip of the indenter



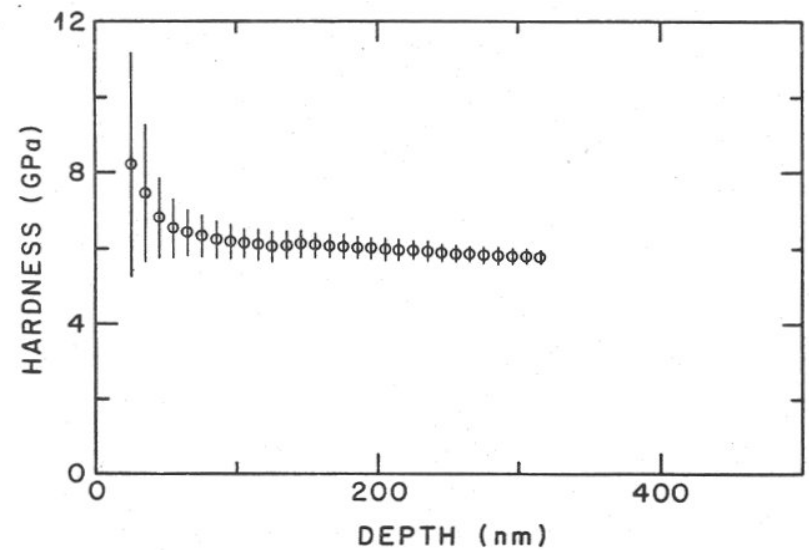
Load versus depth for electropolished nickel (Pethica et al 1983)



Load versus depth for mechanically polished silicon (Pethica et al 1983)



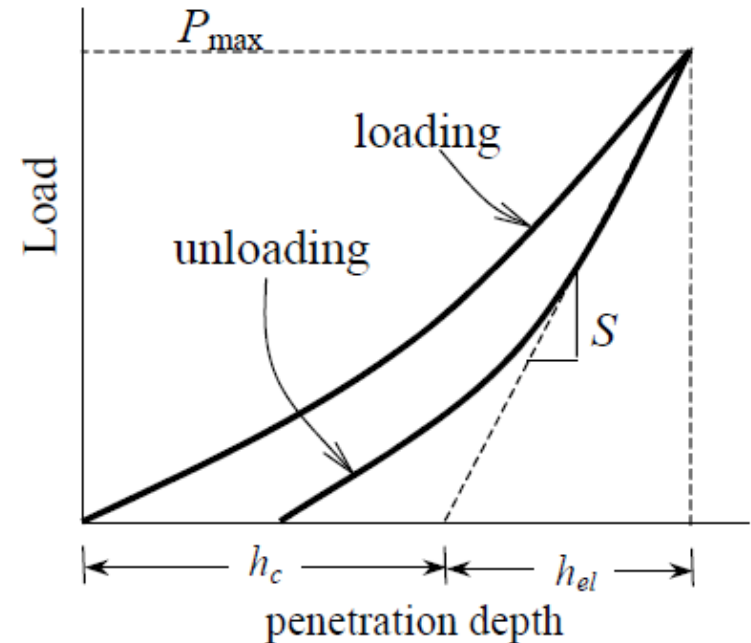
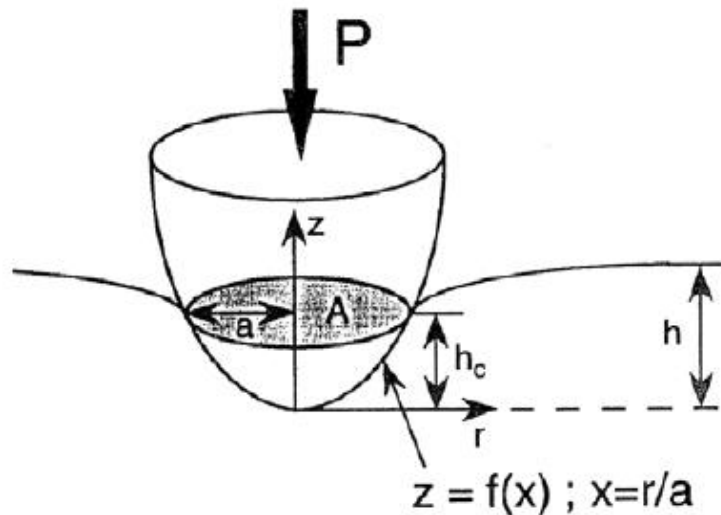
Hardness versus maximum penetration depth for electropolished nickel (Pethica et al 1983)



Hardness versus maximum penetration depth for mechanically polished silicon (Pethica et al 1983)

■ Elastic properties calculated from elastic loading

- Sneddon's solution for axisymmetric tips (1965)



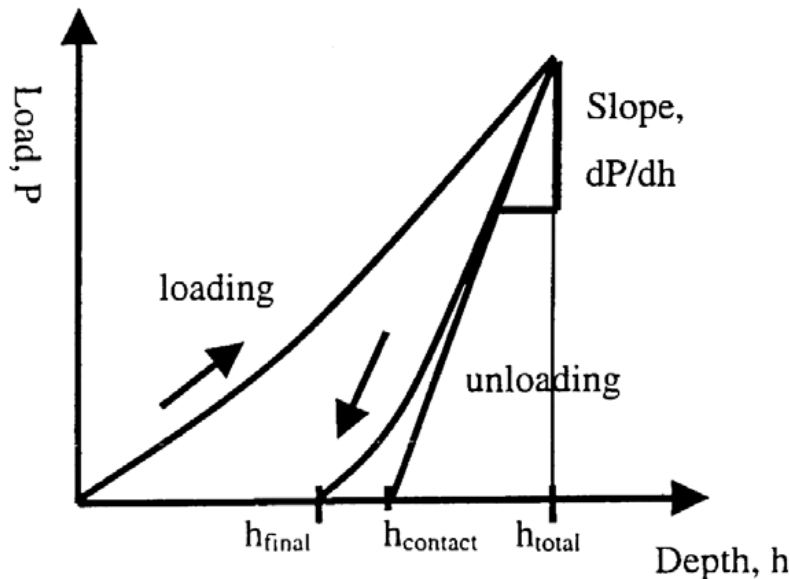
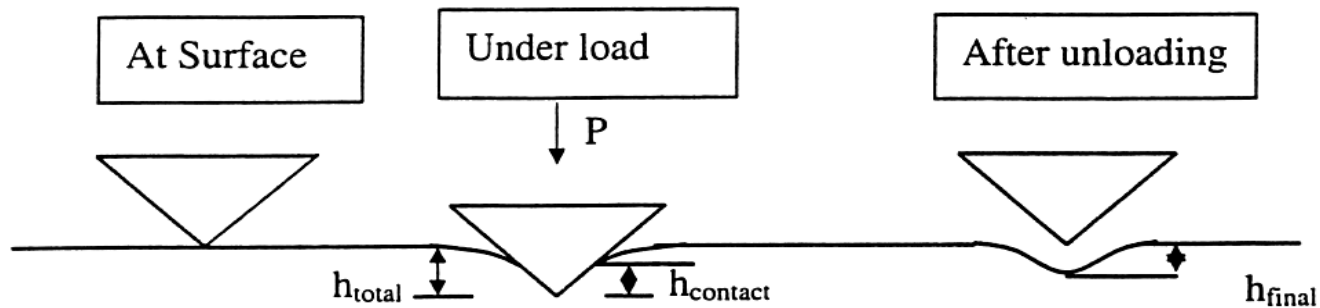
$$S = \frac{dP}{dh} = \frac{2\beta}{\sqrt{\pi}} E_{eff} \sqrt{A_p}; \quad A_p = \alpha h_c^2; \quad h_c = 2h/\pi$$

S : stiffness; A_p : projected contact area; E_{eff} : effective modulus

α, β : factors depending on tip geometry

- **Doerner & Nix (D-N) Analysis (1986)**

- *Assumptions:*
 1. Constant contact area during initial unloading
 2. Initial unloading is linear (common for most materials in the 1/3 of the unloading curve)



- *Calculation*

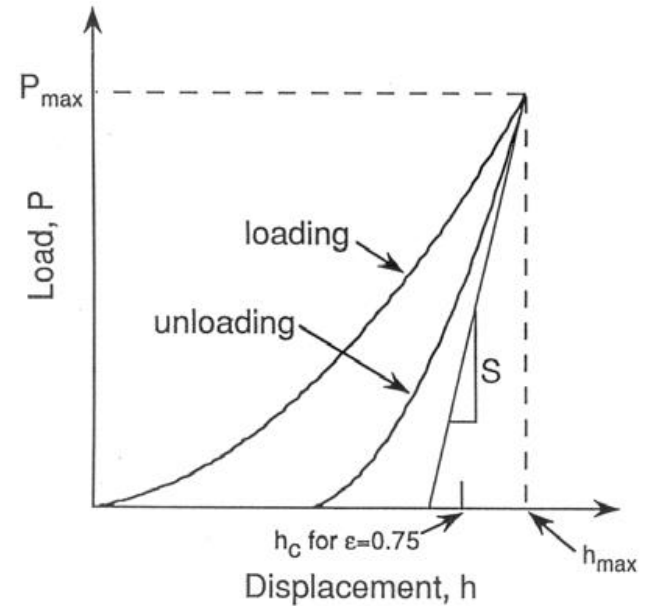
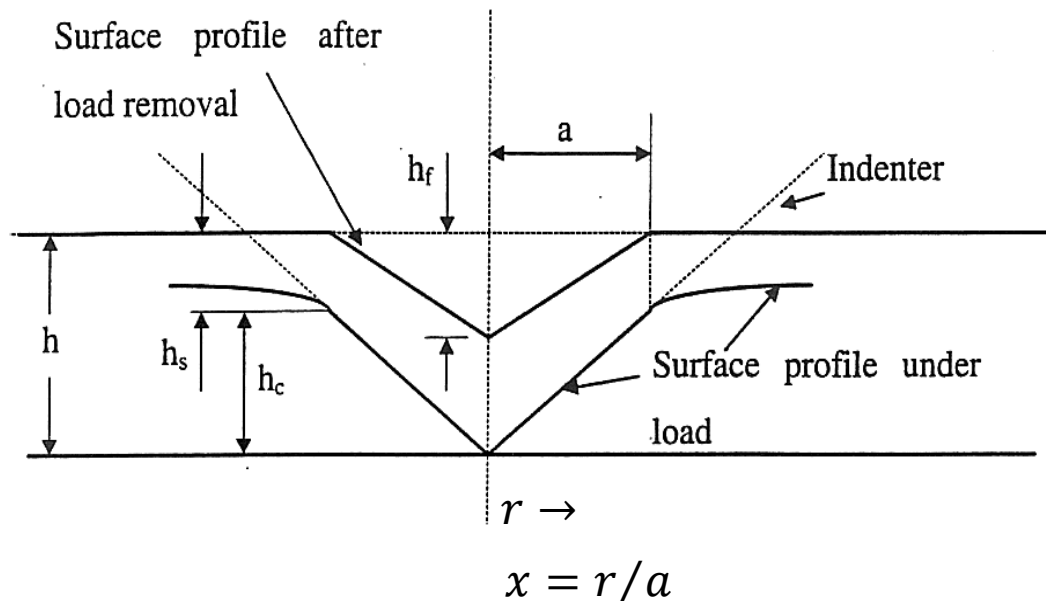
Linear fitting to the upper 1/3 of the unloading curve $\Rightarrow S$ & $h_c \Rightarrow$ contact surface area A_c (a function of h_c).

Then from Sneddon's formula:

$$E_{eff} = \frac{\sqrt{\pi}}{2\beta} \frac{S}{\sqrt{A_c}}$$

• *Oliver & Pharr (O-P) Analysis (1992)*

- Fitting of the unloading curve with a power-law relation $P = B(h - h_f)^m$
- In addition to elastic, plastic deformation is also considered

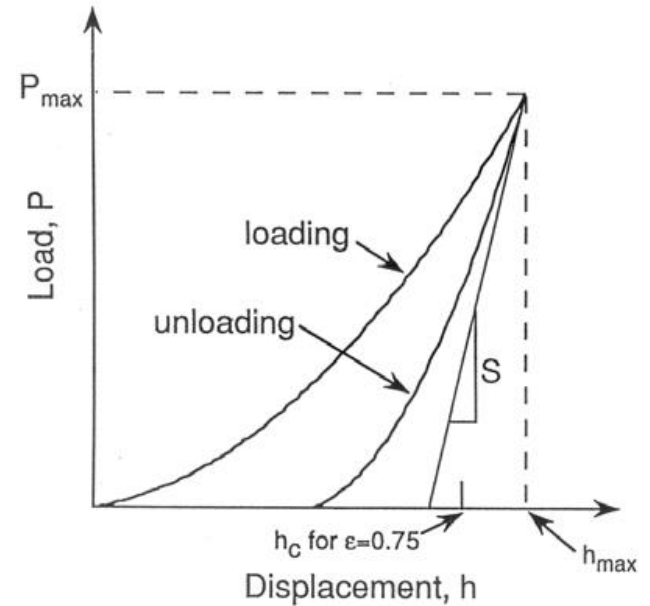
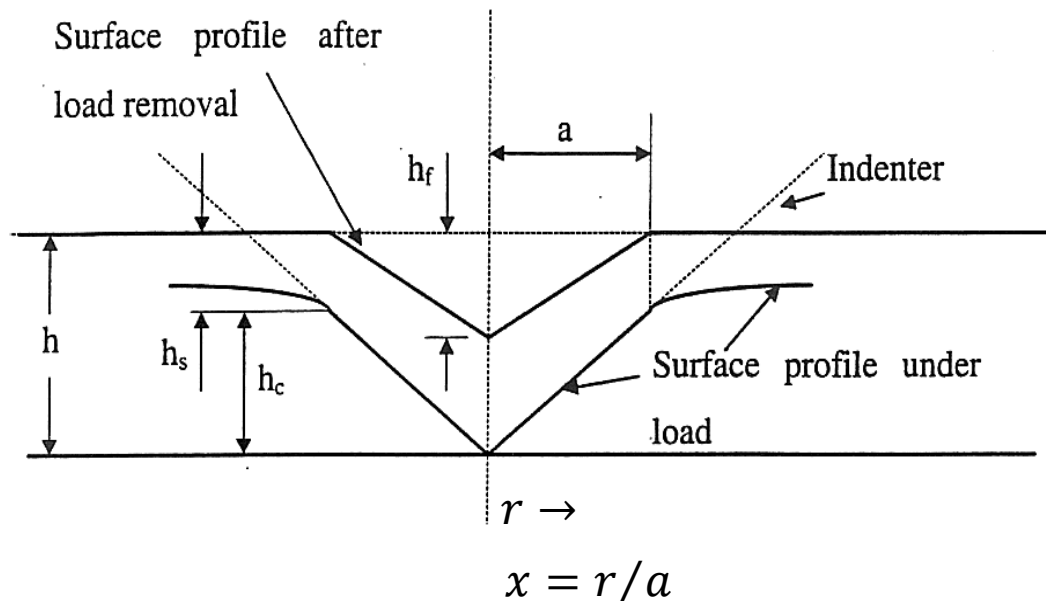


- *Definitions*

$$\left. \begin{array}{l} \text{Total displacement:} \quad u_t = h - h_c x \\ \text{Residual displacement:} \quad u_p = h_f - h_f x \\ \text{Elastic displacement:} \quad u_e = u_t - u_p \end{array} \right\} \Rightarrow u_e = (h - h_f) - (h_c - h_f)x$$

• *Oliver & Pharr (O-P) Analysis (1992)*

- Fitting of the unloading curve with a power-law relation $P = B(h - h_f)^m$
- In addition to elastic, plastic deformation is also considered



- *Definitions*

$$\left. \begin{array}{l} \text{Total displacement:} \quad u_t = h - h_c x \\ \text{Residual displacement:} \quad u_p = h_f - h_f x \\ \text{Elastic displacement:} \quad u_e = u_t - u_p \end{array} \right\} \Rightarrow u_e = (h - h_f) - (h_c - h_f)x$$

USE OF GRADIENT ELASTICITY IN INDENTATION

■ Motivation

• Problems in Nanoindentation Test modeling

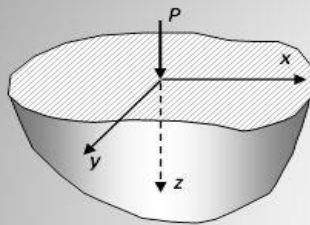
- Elastic properties calculated from “elastic unloading” rather than from elastic loading
- Use of Sneddon’s solutions of axisymmetric tips for non-axisymmetric ones (Berkovich, Vickers)
- Use of inappropriate geometrical assumptions
- A 3D problem considered to be a 1D problem
- Elastic Modulus and Hardness depending on depth (ISE)

■ A newer approach for Nanoindentation

• Introduction of initial elasticity under any indenter tip

The displacement field of the material under the indenter before any plasticity takes place, is given by the Boussinesq's elasticity solution

Comparison of Flamant Results with 3-D Theory - Boussinesq's Problem



Free Surface Displacements

$$u_x(R, 0) = \frac{P(1-\nu)}{2\pi\mu R}$$

Corresponding 2-D Results

$$u_\theta(r, 0) = -\frac{P}{\pi E} [(1+\nu) + 2 \log r]$$

3-D Solution eliminates the unbounded far-field behavior

Cartesian Solution

$$u = \frac{Px}{4\pi\mu R} \left(\frac{z}{R^2} - \frac{1-2\nu}{R+z} \right), \quad v = \frac{Py}{4\pi\mu R} \left(\frac{z}{R^2} - \frac{1-2\nu}{R+z} \right), \quad w = \frac{P}{4\pi\mu R} \left(2(1-\nu) + \frac{z^2}{R^2} \right)$$

$$\sigma_x = -\frac{P}{2\pi R^2} \left[\frac{3x^2 z}{R^3} - (1-2\nu) \left(\frac{z}{R} - \frac{R}{R+z} + \frac{x^2(2R+z)}{R(R+z)^2} \right) \right]$$

$$\sigma_y = -\frac{P}{2\pi R^2} \left[\frac{3y^2 z}{R^3} - (1-2\nu) \left(\frac{z}{R} - \frac{R}{R+z} + \frac{y^2(2R+z)}{R(R+z)^2} \right) \right]$$

$$\sigma_z = -\frac{3Pz^3}{2\pi R^5}, \quad \tau_{xy} = -\frac{P}{2\pi R^2} \left[\frac{3xyz}{R^3} - \frac{(1-2\nu)(2R+z)xy}{R(R+z)^2} \right]$$

$$\tau_{yz} = -\frac{3Pyz^2}{2\pi R^5}, \quad \tau_{zx} = -\frac{3Pxz^2}{2\pi R^5}$$

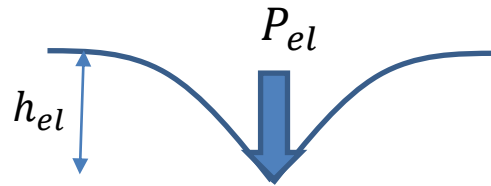
Cylindrical Solution

$$u_r = \frac{P}{4\pi\mu R} \left[\frac{rz}{R^2} - \frac{(1-2\nu)r}{R+z} \right], \quad \sigma_r = \frac{P}{2\pi R^2} \left[-\frac{3r^2 z}{R^3} + \frac{(1-2\nu)R}{R+z} \right]$$

$$u_z = \frac{P}{4\pi\mu R} \left[2(1-\nu) + \frac{z^2}{R^2} \right], \quad \sigma_\theta = \frac{(1-2\nu)P}{2\pi R^2} \left[\frac{z}{R} - \frac{R}{R+z} \right]$$

$$u_\theta = 0, \quad \sigma_z = -\frac{3Pz^3}{2\pi R^5}, \quad \tau_{rz} = -\frac{3Prz^2}{2\pi R^5}$$

- **Boussinesq's elasticity solution**



Elastic problem

Elastic Displacement Field (cartesian coordinates)

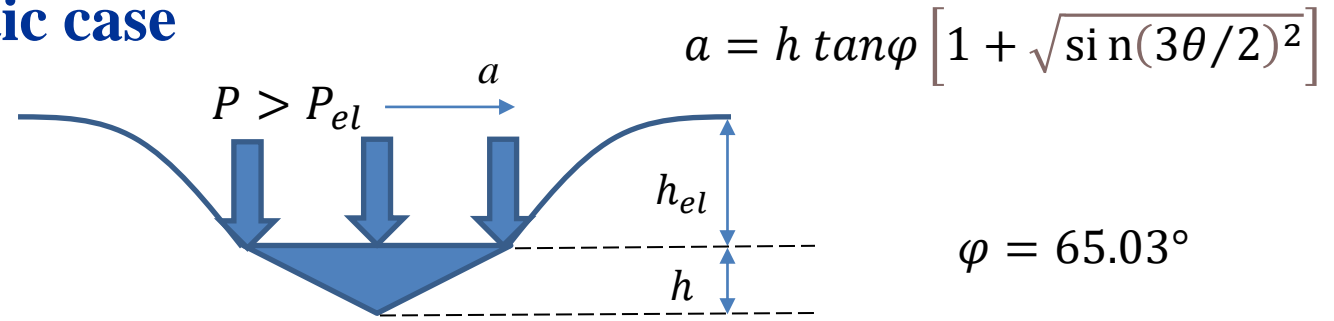
$$u_x = \frac{Px}{4\pi\mu R} \left(\frac{z}{R^2} - \frac{1-2\nu}{R+z} \right), u_y = \frac{Py}{4\pi\mu R} \left(\frac{z}{R^2} - \frac{1-2\nu}{R+z} \right), u_z = \frac{P}{4\pi\mu R} \left(\frac{z}{R^2} + 2(1-\nu) \right)$$

Elastic Displacement Field (cylindrical coordinates)

$$u_r = \frac{P}{4\pi\mu R} \left(\frac{rz}{R^2} - \frac{r(1-2\nu)}{R+z} \right), \quad u_\theta = 0, \quad u_z = \frac{P}{4\pi\mu R} \left(\frac{z^2}{R^2} + 2(1-\nu) \right)$$

$$\left(R = \sqrt{x^2 + y^2 + z^2} = \sqrt{r^2 + z^2} \right)$$

- **Elastoplastic case**



Elastoplastic problem

Berkovich Displacement Field (cylindrical coordinates)

$$u_z^{berk} = ((h + h_{el} - z) \sin \varphi - r \cos \varphi) \sin \varphi, u_r^{berk} = \frac{u_z^{berk} (1 + |\sin \frac{3\theta}{2}|)}{\tan \varphi}, u_\theta^{berk} = 0$$

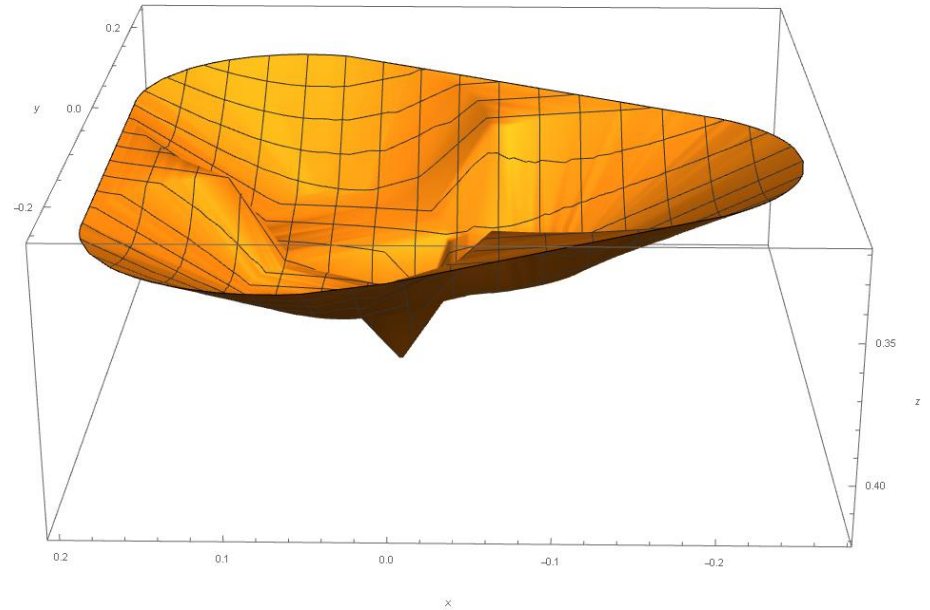
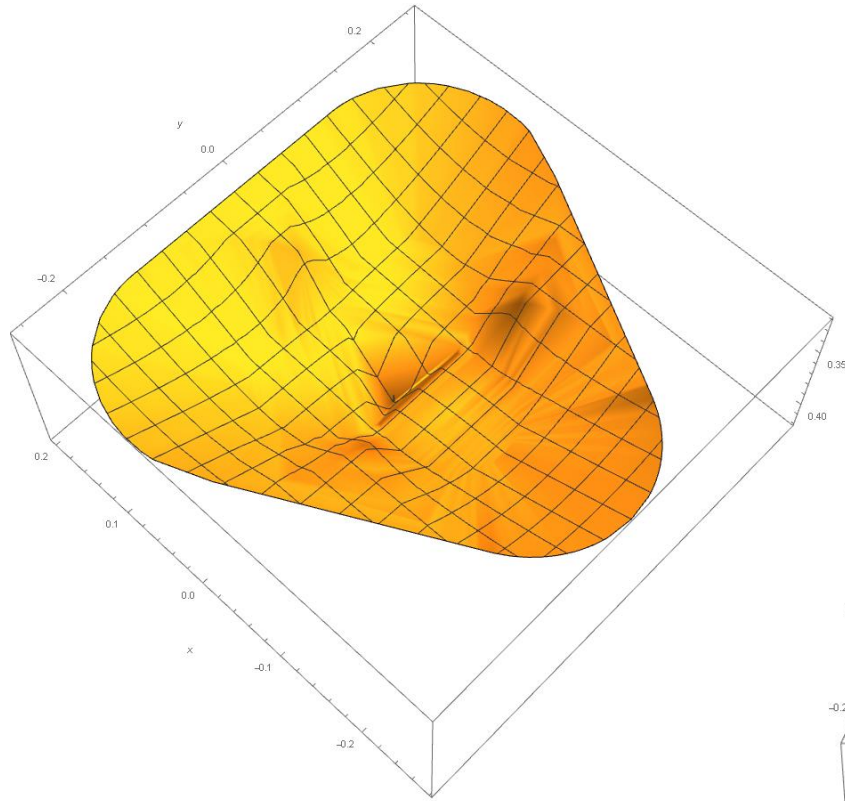
Total Displacement Field (cylindrical coordinates)

$$u_r^{tot} = u_r \Big|_{r \rightarrow r+a} + u_r^{berk}$$

$$u_\theta^{tot} = u_\theta \Big|_{r \rightarrow r+a} + u_\theta^{berk} = 0$$

$$u_z^{tot} = u_z \Big|_{r \rightarrow r+a} + u_z^{berk}$$

- **Displacement of a Berkovich tip taking elasticity into account**



Displacement field (cartesian coordinates):

$$u_x = \frac{x \cos^2(\varphi) (\sqrt{\sin^2(\frac{3}{2} \tan^{-1}(x, y)) + 1} (\sin^2(\varphi) (h + h_{el} - z) - \cos^2(\varphi) \sqrt{x^2 + y^2})}{\sqrt{x^2 + y^2}} + \frac{h_{el}^2 x (\frac{2\nu - 1}{\sqrt{x^2 + y^2 + z^2} + z} + \frac{z}{x^2 + y^2 + z^2})}{2(1 - \nu) \sqrt{x^2 + y^2 + z^2}}$$

$$u_y = \frac{y \cos^2(\varphi) (\sqrt{\sin^2(\frac{3}{2} \tan^{-1}(x, y)) + 1} (\sin^2(\varphi) (h + h_{el} - z) - \cos^2(\varphi) \sqrt{x^2 + y^2})}{\sqrt{x^2 + y^2}} + \frac{h_{el}^2 y (\frac{2\nu - 1}{\sqrt{x^2 + y^2 + z^2} + z} + \frac{z}{x^2 + y^2 + z^2})}{2(1 - \nu) \sqrt{x^2 + y^2 + z^2}}$$

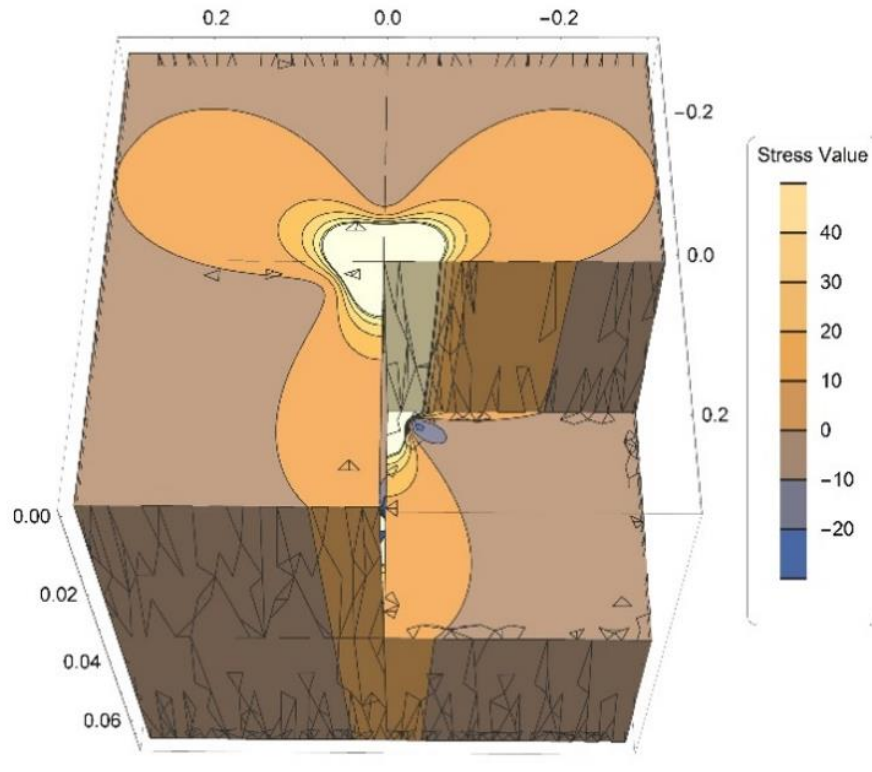
$$u_z = \sin^2(\varphi) (h + h_{el} - z) + \frac{h_{el}^2 (x^2 + y^2 + (\frac{1}{2 - 2\nu} + 1) z^2)}{(x^2 + y^2 + z^2)^{3/2}} - \sin^2(\varphi) \cos^2(\varphi) \sqrt{x^2 + y^2}$$

Strain / Stress fields (cartesian coordinates):

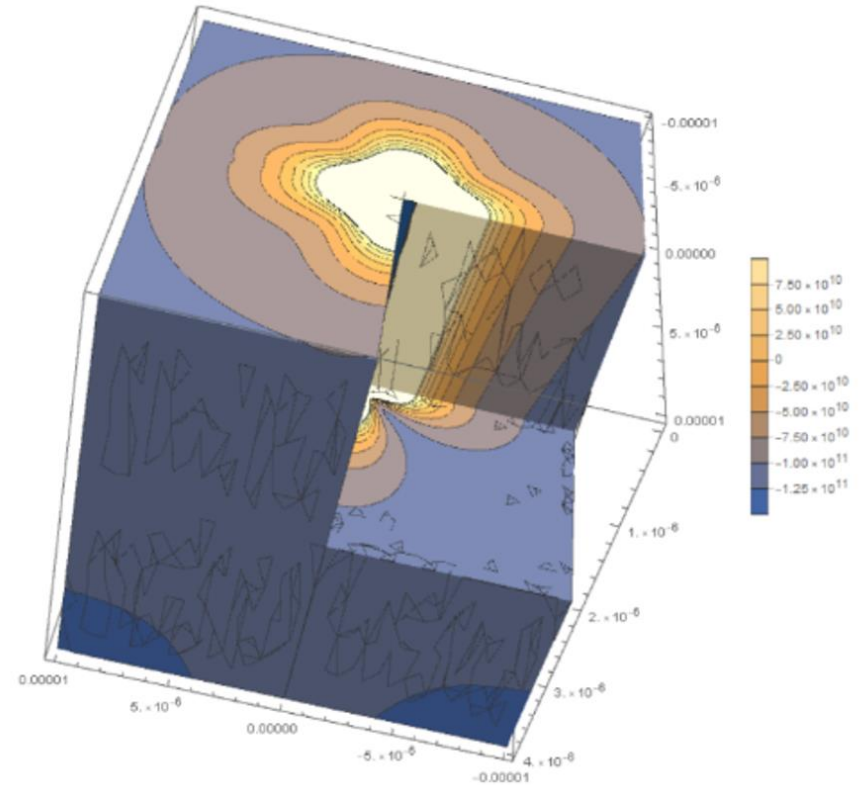
$$\mathbf{E} = \frac{1}{2} (\mathbf{F}^T \mathbf{F} - \mathbf{I}) \Rightarrow E_{ij} = \begin{bmatrix} E_{xx} & E_{xy} & E_{xz} \\ E_{yx} & E_{yy} & E_{yz} \\ E_{zx} & E_{zy} & E_{zz} \end{bmatrix} = \dots = f(\mu, h_{el}, c)$$

$$\boldsymbol{\sigma} = \lambda \text{tr}(\mathbf{E}) \mathbf{1} + 2\mu \mathbf{E} + c \nabla^2 [\lambda \text{tr}(\mathbf{E}) \mathbf{1} + 2\mu \mathbf{E}] = \dots$$

- 3D contour plots - σ_{zz}^{grad}



Berkovich

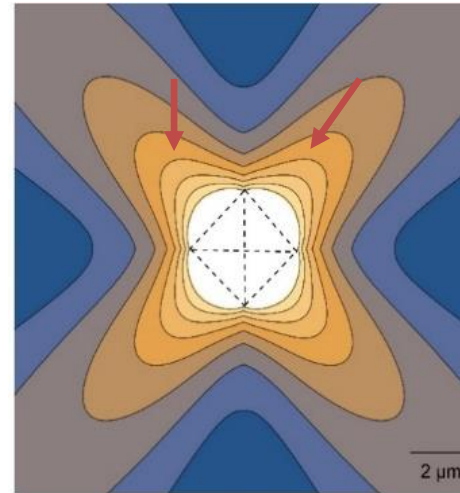
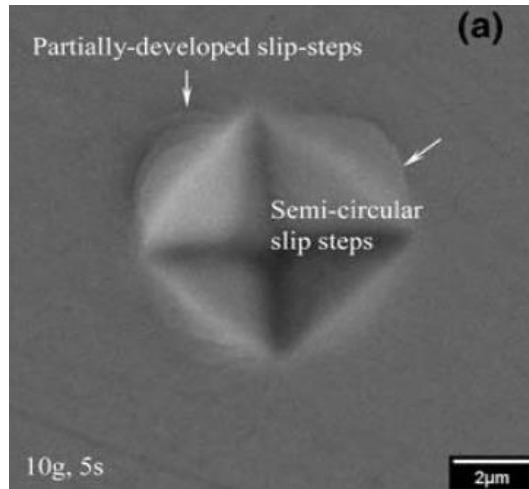


Vickers

■ Shear bands during indentation

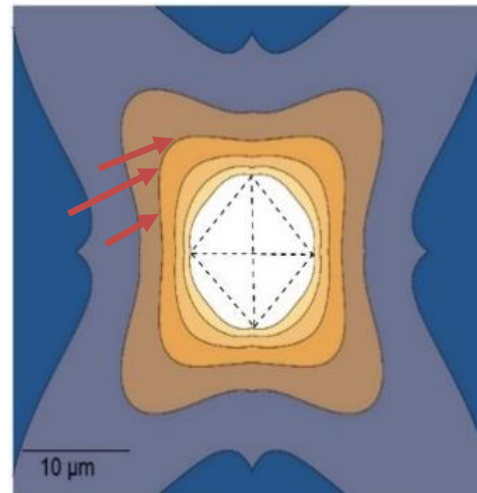
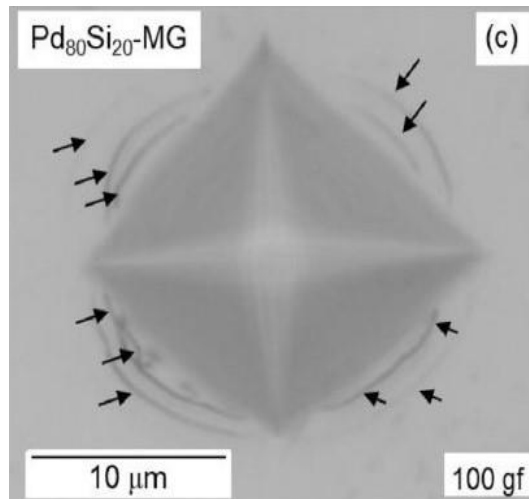
Zhang et al. (2005)

Vitreloy 106



Sharma et al. (2021)

Pd₈₀Si₂₀

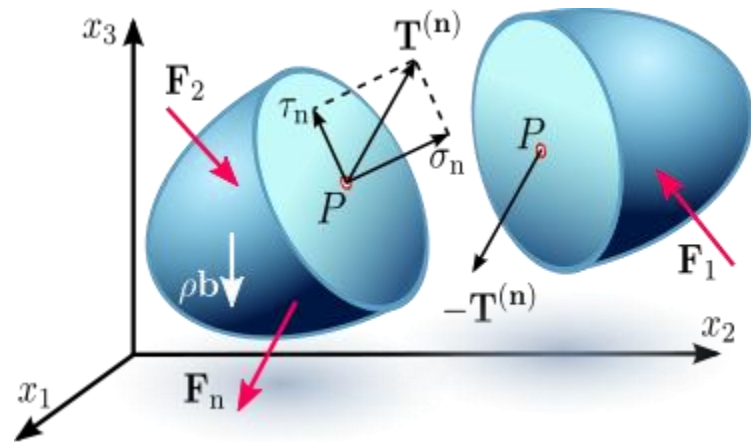


Kampouris et al. (2022)

- **Elastic modulus calculation**

Traction Vector

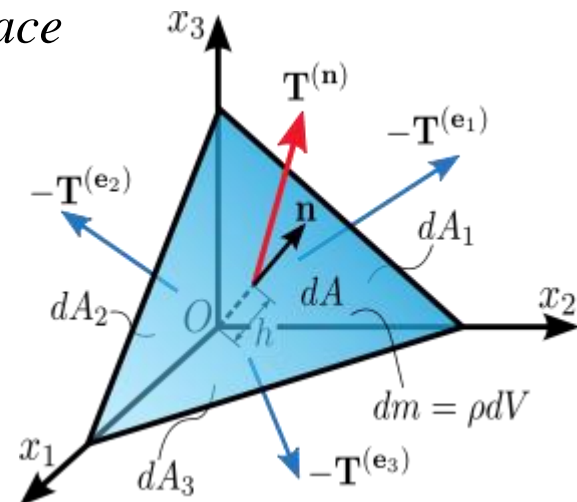
$$\mathbf{T}^{(\mathbf{n})} = \mathbf{n} \cdot \boldsymbol{\sigma}$$



Traction Vector perpendicular to indenter tip face

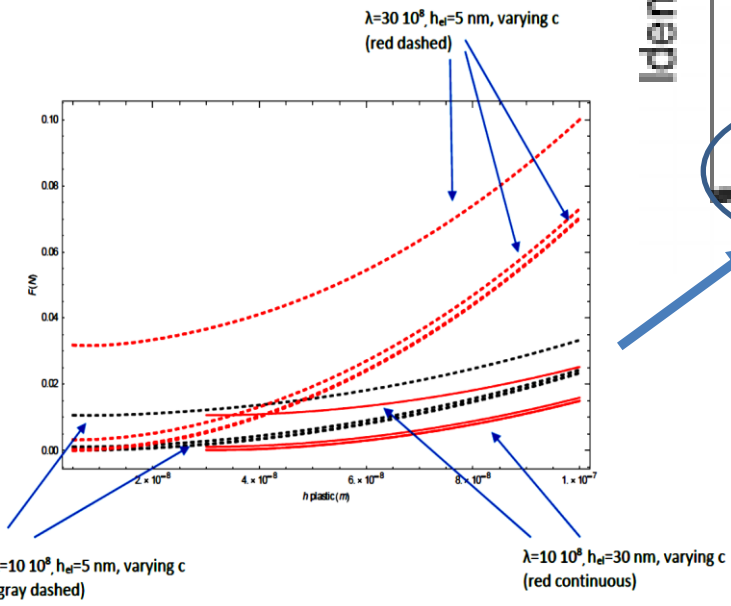
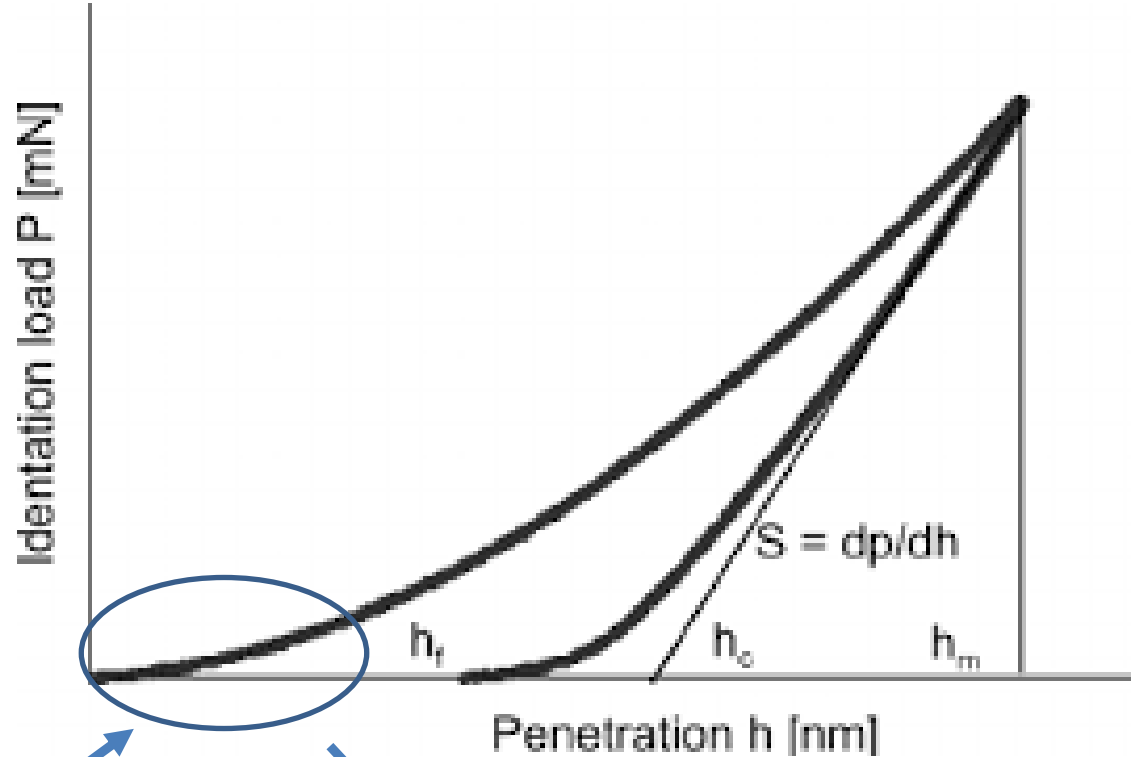
$$\mathbf{T}^{(\mathbf{n})} = \mathbf{n}_{face} \cdot \boldsymbol{\sigma}_{elastoplastic}$$

$$|\mathbf{T}^{(\mathbf{n})}| = \dots = f(\lambda, h_{el}, c)$$



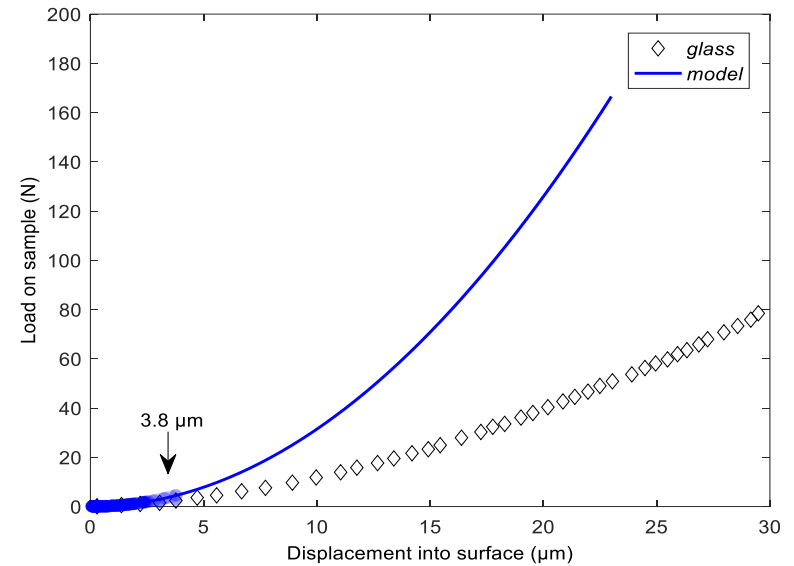
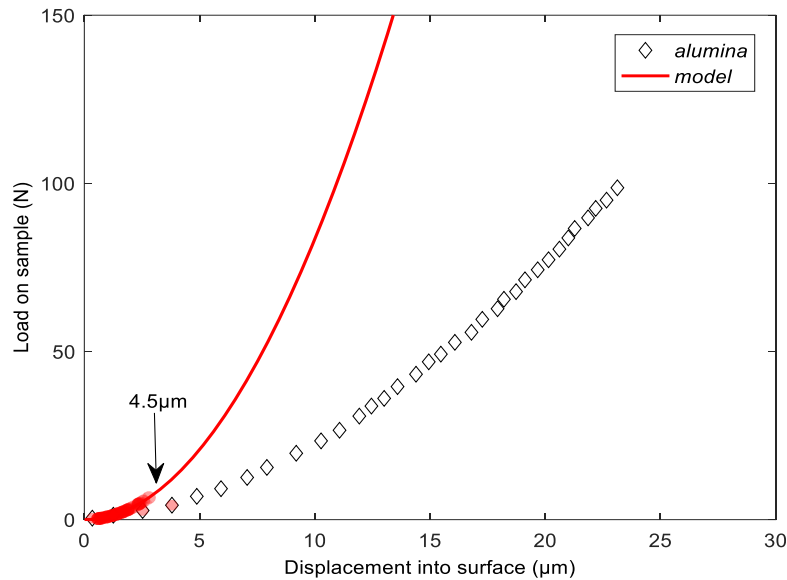
- Elastic modulus calculation

$$|T^{(n)}| A_{face} = \dots = P(\lambda, h_{el}, c)$$



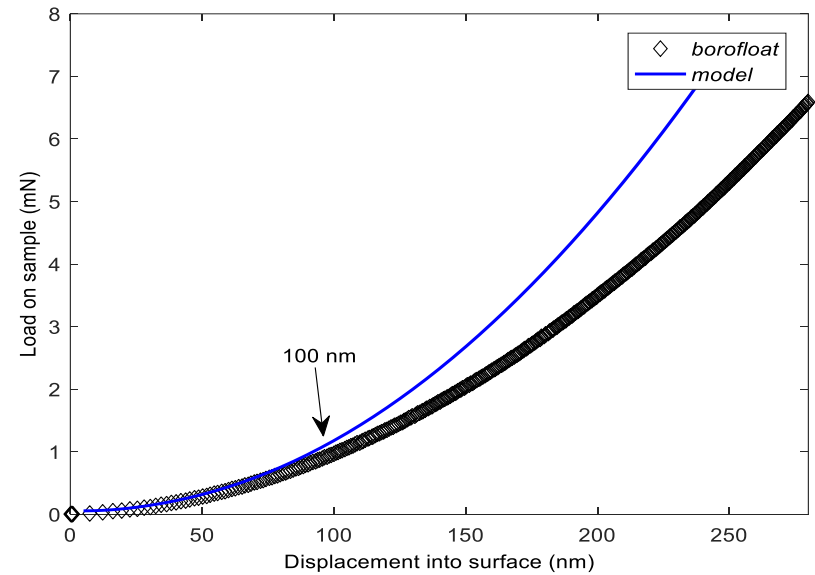
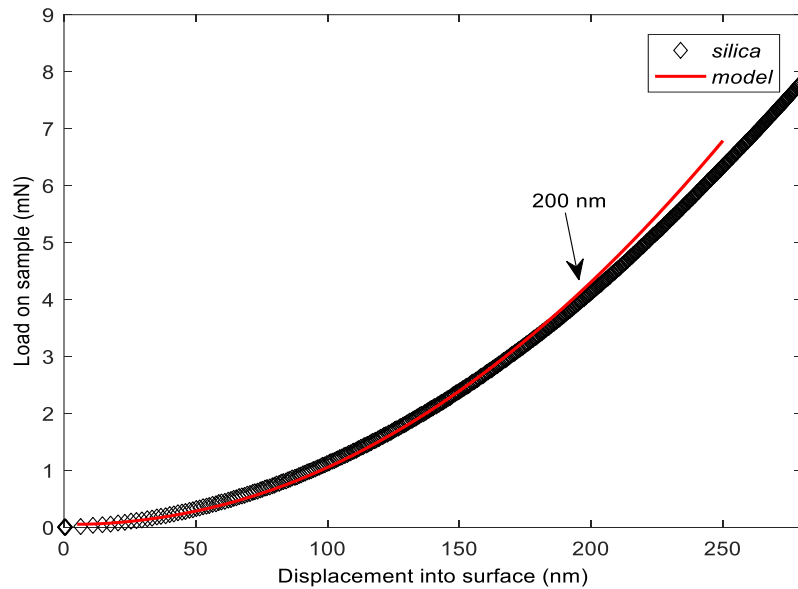
$\lambda \rightarrow E$
 $h_{el} \rightarrow H$

- Application on Alumina and Glass Experimental Data



	Alumina	Glass
ν	0.21	0.23
h_{el} (nm)	10	10
c (m^2)	$2 \cdot 10^{-16}$	$2 \cdot 10^{-16}$
φ	68°	68°
E (GPa)	215	72

- Application on Silica and Borofloat Experimental Data



	SiO₂	Borofloat
ν	0.17	0.2
hel (nm)	5	5
c (m ²)	10 ⁻¹⁸	10 ⁻¹⁸
φ	65.03°	65.03°
E (GPa)	69.2	62